

Chiral symmetry breaking via crystallization of the glycine and α -amino acid system: a mathematical model

Celia Blanco^{1,*} and David Hochberg^{1,†}

¹*Centro de Astrobiología (CSIC-INTA), Carretera Ajalvir Kilómetro 4, 28850 Torrejón de Ardoz, Madrid, Spain*

We introduce and numerically solve a mathematical model of the experimentally established mechanisms responsible for the symmetry breaking transition observed in the chiral crystallization experiments reported by I. Weissbuch, L. Addadi, L. Leiserowitz and M. Lahav, *J. Am. Chem. Soc.* **110** (1988), 561-567. The mathematical model is based on five basic processes: (1) The formation of achiral glycine clusters in solution, (2) The nucleation of oriented glycine crystals at the air/water interface in the presence of hydrophobic amino acids, (3) A kinetic orienting effect which inhibits crystal growth, (4) The enantioselective occlusion of the amino acids from solution, and (5) The growth of oriented host glycine crystals at the interface. We translate these processes into differential rate equations. We first study the model with the orienting process (2) without (3) and then combine both allowing us to make detailed comparisons of both orienting effects which actually act in unison in the experiment. Numerical results indicate that the model can yield a high percentage orientation of the mixed crystals at the interface and the consequent resolution of the initially racemic mixture of amino acids in solution. The model thus leads to separation of enantiomeric territories, the generation and amplification of optical activity by enantioselective occlusion of chiral additives through chiral surfaces of glycine crystals.

I. INTRODUCTION

Theoretical proposals for prebiotic chemistry suggest that homochirality emerged in nature in abiotic times via deterministic or chance mechanisms [1]. The abiotic scenario for the emergence of single homochirality in the biological world implies that single asymmetry could have emerged provided a small fluctuation from the racemic state can be amplified to a state useful for biotic evolution. For this reason, experiments that can demonstrate the feasibility of stochastic mirror symmetry breaking involving the self assembly of molecular clusters, and in possible conjunction with interface effects, are particularly important. This is because, once generated by chance or an initial chiral fluctuation, the chirality can then be preserved and transmitted to the rest of the system provided that the symmetry breaking step is coupled to a sequential step of efficient amplification via self-replication reactions. Some relevant features common to such systems are that they take into account the small fluctuations about the racemic state and that they display nonlinear kinetic effects. Stochastic scenarios are theoretically well understood[2, 3] and are experimentally feasible in the laboratory [4].

Among the experiments dedicated to exploring chance mechanisms in chirality, a particularly noteworthy and important result with a marked relevance for prebiotic chemistry stands out. The experiment we are interested in modeling here was reported some years ago by the Rehovot group which dealt with an autocatalytic process for the resolution of racemic α -amino acids within crystals of glycine grown at the air/solution interface [5, 6]. They applied cooperative crystallization processes for the spontaneous separation of racemic mixtures of α -amino acids rich with glycine into optically pure enantiomers. Their experimental model involves slow evaporation of aqueous solutions of the centrosymmetric form of glycine containing racemic mixtures of α -amino acids. Due to the unique crystal structure of glycine, all chiral D-amino acids except for proline are occluded within the crystal through the (010) face, whereas the L-amino acids are occluded through the (0 $\bar{1}$ 0) face. Glycine crystals float in solution, so that only one face is available for growth. Thus when glycine crystals are grown at the air/water interface in the presence of DL-amino acids, only one of its enantiotopic faces, say (010), is exposed to the solution and so picks up only the D-amino acid together with glycine. By symmetry, crystals exposing their (0 $\bar{1}$ 0) face towards solution occlude only the L-enantiomers. Now, if by *chance* a single or small number of oriented glycine crystals grow initially at the interface, the bulk solution will be enhanced with the amino acid of one handedness. The preservation and transmission of the chirality generated by chance of the original *Adam*[23] crystal means that new crystals grown at later stages at this interface must adopt the same orientation. There are two proven ways this is achieved[5, 6]: by means of an (i) hydrophobic effect and (ii) by a kinetic inhibition effect. Regarding the first effect, if the solution contains hydrophobic amino acids, these tend

*Electronic address: blancodtc@cab.inta-csic.es

†Electronic address: hochbergd@cab.inta-csic.es

to accumulate at the interface forming two-dimensional domains acting as templates for the oriented crystallization of the glycine crystals. Thus, the L-amino acids induce crystallization of floating glycine crystals exposing their (010) face towards solution and these occlude only the D-amino acids. This asymmetric induction has been established experimentally[5, 7]. As for the second effect, this comprises an enantioselective inhibition of the glycine nuclei by the amino acids present in solution (these can be both partially dissolved hydrophobic as well as hydrophilic amino acids). This independent effect was proven experimentally by achieving complete orientation of the floating glycine nuclei when grown in the presence of DL-leucine and hydrophilic L amino acids. The presence of the DL-leucine is to ensure nucleation of floating glycine crystals exposing either enantiotopic face towards solution in a 1 : 1 ratio whereas increasing the concentration of the hydrophilic amino acid additives inhibited the glycine nuclei exposing their (0 $\bar{1}$ 0) face and so prevented their further growth. These hydrophilic amino acids inhibit the crystal nuclei from growing and developing into macroscopic crystals[8]. Both the hydrophobic and kinetic effects act cooperatively in the same direction in that they both contribute to the territorial segregation of the enantiomers.

The overall experimental process can be summarized by the following steps (Figure 1)[6],[4]:(i) mirror symmetry breaking via the enantioselective occlusion of one of the enantiomers of the racemic α -amino acids within crystals of glycine grown at the air/solution interface, (ii) the oriented crystal formed at the interface operates as a seed for further occlusion of amino acids of the same handedness, (iii) the amplification experiments comprises self-aggregation of hydrophobic α -amino acids into chiral clusters that operate as templates for an oriented crystallization of fresh crystals of glycine. (i.e, the hydrophobic effect), and (iv) enantioselective inhibition of embryonic nuclei of glycine generated at the air/solution interface by the water soluble α -amino acids formed in excess during the process. (i.e., the kinetic effect). The fundamental relevance of this experiment is that it provides a simple chemical model for the

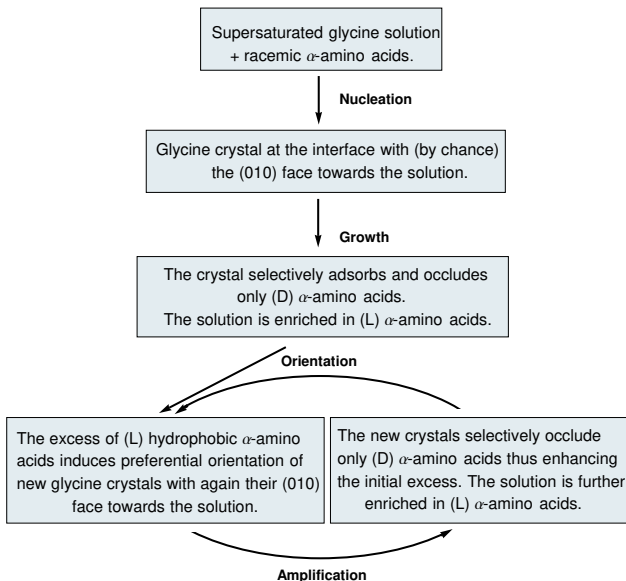


FIG. 1: The overall process of mirror symmetry breaking and amplification. Scheme adapted from references[4, 6].

generation and amplification of optically active amino acids in prebiotic conditions. They used a centrosymmetric crystal structure of glycine, which is the only achiral amino acid and is the major component found in modern prebiotic synthesis experiments[9]. The possibility to maintain and propagate the same chirality to the entire system can lead in principle to a complete separation of enantiomeric territories and subsequent optical activity. The enantiomeric resolution and symmetry breaking is achieved without the need to input mechanical energy: in particular there is no need for stirring [10] nor grinding [11], and it involves only amino acids which have an immediate and obvious relevance for prebiotic chemistry. That the experiment dispenses with the need for mechanical energy is a most remarkable feature. Some provisional explanations of how this is achieved are offered in the final conclusions.

In spite of its importance, we are unaware of any prior attempts to offer a mathematical model for describing the reported phenomenon. The purpose of this paper is to provide a simple and minimal mathematical model of the key processes to further elucidate the mechanisms responsible for the observed symmetry breaking and to gain further understanding of the experiment itself. Our aim is to describe the resolution process by means of a kinetic mean field model in which we include only the minimal essentials responsible for the crystal growth and the symmetry breaking

phenomenon. The mathematical model is based on five basic processes that parallel closely those that have been established experimentally: (1) The formation of achiral glycine clusters in solution, (2) The nucleation of oriented glycine crystals at the air/water interface in the presence of hydrophobic amino acids, (3) A kinetic orienting effect which inhibits crystal growth from embryonic crystals, (4) the enantioselective occlusion of the amino acids from solution, and (5) the growth of oriented host glycine crystals at the interface via glycine up-take. We first introduce the model with only the hydrophobic orienting process (2) as an approximation to the complete model. This is a justifiable first approximation to consider given that the experimental results prove that this effect plays a *dominant* role in the orientation of the glycine crystals [6]. The major simplifications are introduced at this stage and we use this model to prove that the symmetric state is unstable. We then include both effects (2) and (3) in a complete final version allowing us to make detailed comparisons of both effects which actually act in unison in the experiment. We present numerical studies of the effects of varying amounts of both the hydrophobic and hydrophilic additives on the orientation of the floating glycine crystals, as was originally considered in the experiments. The results indicate that our simple model can yield a high percentage orientation of the glycine-host plus guest-enantiomer mixed crystals at the interface with the consequent resolution of the initially racemic mixture of amino acids in solution. The mathematical model thus leads to separation of enantiomeric territories, the generation and amplification of optical activity by enantioselective occlusion of chiral additives through chiral surfaces of glycine crystals.

II. REACTION MODEL

A. Preliminaries

A full experimental account is given in the two papers [5, 6] and is reviewed [4, 12] together the references therein; and these serve as basic inspiration and background guide for elaborating the model we present in this paper.

Following the experimental conditions, we consider a supersaturated solution of glycine and racemic α amino acids. The glycine monomers and clusters in solution will be denoted by A_1 and A_r , respectively, the cluster being made up from r -monomer units. It is reasonable to assume that a typical glycine cluster size should exist $\langle r \rangle = M$ for M monomeric units. This is the average size of the primary nucleation or seed crystal which can then precipitate at the air/water interface where it will, in the *presence* of hydrophobic D and L -amino acids, assume one of two unique orientations [6]. Let X_M and Y_M denote the two possible orientations of the glycine crystal floating at the interface: X stands for the (010) enantiotopic face exposed to solution and Y for the other ($0\bar{1}0$) enantiotopic face exposed to solution. The D and L denote the two amino acid enantiomers. For a strictly racemic solution of the amino acids, (which is of course impossible to realize experimentally [13]), we would expect an equal $X : Y = 1 : 1$ proportion of the two glycine crystal orientations at the interface. However, if for example there is an imbalance in the initial concentrations, say $L > D$, then more of the Y -oriented crystals will be precipitated. Likewise for the X -oriented crystals if instead $L < D$.

Next, we consider the enantioselective occlusion of the amino acid into the host glycine crystals: recall only the (010) face of the glycine crystal can occlude the D amino acid whereas only the ($0\bar{1}0$) face can occlude the L amino acid; see Figure 1. It will prove instructive to first write down a kind of “microscopic” model which contemplates all kinds of crystal aggregations growing from both glycine take-up and the amino acid occlusion and with cluster size dependent rates and then simplify by taking the reaction rates independent of cluster size, and assuming only cluster-monomer aggregation. We will not consider fragmentation in any case: we assume irreversible steps from the outset. Since the hydrophobic effect dominates over the kinetic one [6], we will consider this one first.

B. Model based on the hydrophobic crystal orientation effect

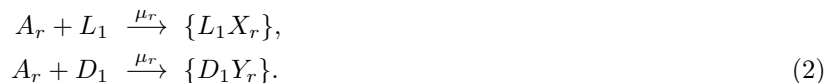
We now introduce the explicit processes to be included in the mathematical model. We transcribe the scheme in Figure 1 into reaction steps. Simplifications will follow later on in order to obtain what we will consider as a minimal model leading to mirror symmetry breaking.

The formation of glycine aggregates/clusters in solution. The achiral molecules of glycine in solution combine pairwise to yield achiral glycine clusters in solution, where r, s denote number of monomers in the cluster and $\delta_{r,s}$ is the cluster size dependent rate constant:



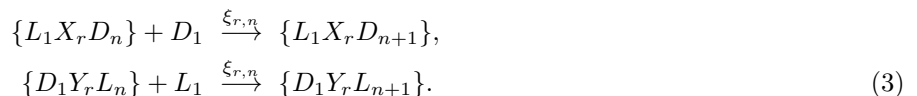
We assume this step is irreversible, there is no fragmentation of the glycine aggregate. Below, we simplify this so that only dimers are formed ($r = 1, s = 1$) [14].

Nucleation of oriented glycine crystals at the air/water interface in presence of hydrophobic LD-amino acids. The hydrophobic amino acid at the interface acts as a nucleator or seed (see also Scheme 5 in [4]):



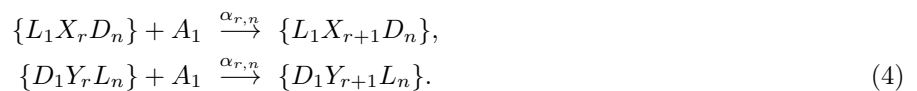
Here and henceforth, the brackets denote the solid phase. This process occurs at the rate μ_r . The two enantiotopic crystal faces exposed to the solution are denoted by X_r and Y_r , respectively. Realistically, a single leucine or valine molecule cannot serve as a nucleus for the glycine crystallization, instead, several dozens arranged in self-assembly are usually required. However, for the sake of simplicity (and limitations on computational time), we assume that one hydrophobic amino acid monomer is sufficient to trigger the nucleation. Otherwise, we would have to additionally model the formation of the chiral template clusters formed by several hydrophobic amino acids at the interface [7, 15]. This template, whatever its actual size, is incorporated into the growing glycine crystal, but in the face exposed to air. We note that HPLC analysis of the crystals indicates that only minute amounts of the orienting hydrophobic amino acids are occluded through the upward pointing face[5], so our single monomer “template” assumption is not unreasonable and results in a welcome mathematical simplification. Varying the size of the template can only have quantitative but not qualitative effects in so far as mirror symmetry breaking is concerned. Below, we will assume a transition regime, that is, only dimer glycine clusters $r = 2$ get nucleated in this way to form oriented host seeds.

Enantioselective occlusion of the amino acid monomers from solution. Incorporation of the guest molecules (amino acids) into mixed host crystal leading to formation of homochiral mixed crystal. As dictated by the actual experimental results [5], we assume that the X face exposed to solution occludes only the D -amino acids, whereas the Y face occludes only the L -amino acids:



The corresponding rate $\xi_{r,n}$ could depend on both the size r of the glycine host as well as on the number n of previously occluded enantiomers. We assume the oriented host glycine crystal occludes one amino-acid monomer at a time. Crystallographic models suggest that single molecules, not clusters, are incorporated one at a time into the growing crystal. The notation in {...} is such that reading from left to right: the orienting hydrophobic amino acid attached to the face exposed to air, the enantiotopic crystal face exposed to solution (composed of r -glycine monomers) and the number n of occluded amino acids from solution. There is no structural or sequence information implied. Note this step implies that the percent ee of occluded enantiomers per host crystal will be 100%, since each enantiotopic crystal face occludes enantioselectively. This is fully justified by the actual experimental results, see the fourth column of Table I in reference[5].

Growth of the oriented host glycine crystal. Growth of the enantiotopic face exposed to solution by take-up of the achiral glycine monomers from the solution:



The newly acquired monomers adopt the same orientation as their host-face. Assumption: take-up involves one glycine monomer at a time. Here the rate $\alpha_{r,n}$ could in principle depend on r and n .

The above steps give a specific articulation of the Scheme represented in Figure 1. The sequence of pictures in Figure 2 illustrates how the the hydrophobic orienting effect plus the enantioselective occlusion work in tandem to yield resolution and optical activity. For illustrative purposes only, we consider a model in which one hydrophobic amino acid is sufficient to orient crystals at the air/water interface (see the above remarks) and that the crystals can occlude up to two amino acids from the solution. The events are ordered from left to right as indicated by the arrows. Start from a closed system containing a pool of amino acid enantiomers in an initial ratio of $L : D = 10 : 9$ plus an initial concentration of glycine aggregates, Gly. By chance, a glycine aggregate nucleates with its (010) exposed to the solution, this step uses up one hydrophobic L from the solution so now we have $L : D = 9 : 9$. The crystal starts occluding the D monomers from a solution and it therefore becomes enriched in the L enantiomer: $L : D = 9 : 7$. It is more probable that the *next* crystal to be nucleated at the interface will have the same orientation as the Adam crystal. Another L is needed to orient the crystal and so two more D monomers get occluded. The solution is further enriched in the L enantiomer. In the course of time, this yields a cascade mechanism and results in a final configuration with a fully oriented glycine crust with a resolved amino acids for each individual crystal and an optically active solution rich in the L -enantiomer. The finite surface area gets covered by nucleated glycine crystals, and the reactions at the

interface cease when either the maximum number of D 's per crystal are occluded or when they are depleted from the solution.

Note in passing: there no explicit *spatial* or coordinate dependence in this model. We do not explicitly distinguish the interface surface from the bulk solution. We can think of this as a homogeneous two-dimensional model, namely, the two-dimensional air/water interface, with the role of the three-dimensional bulk solution (below the interface) as providing the interface with the new glycine and amino acid molecular building blocks. Also, there is no fragmentation; once formed the crystals do not break up into smaller pieces, the guest molecules stay with their hosts. The real experimental situation is three-dimensional, being composed of an interface plus bulk solution. It is clear that the molecules in solution must diffuse in order to reach the interface. Even the crust formed at the interface is not homogeneous, but is composed of the fusion of many plate-like crystals [6]. We ignore size distribution of the crystals grown at the interface. But for the purposes of obtaining a simple model that leads to experimentally established resolution, these details will not matter. When we treat the complete truncated model below, we will however implement a way to effectively account for the *finite* surface area available for the oriented glycine crystals.

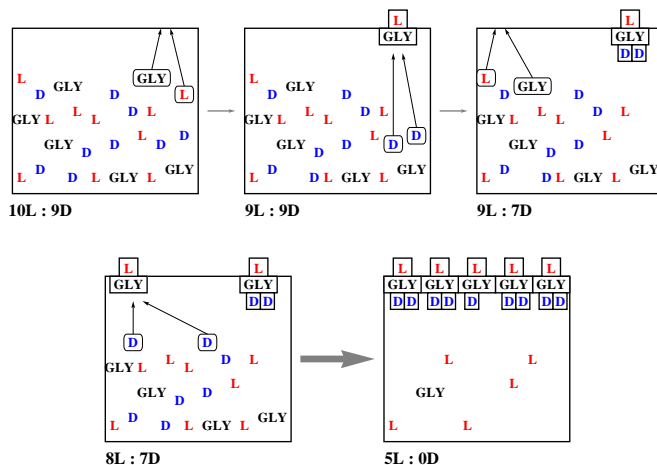


FIG. 2: Simplified schematic representation of our model for the generation and amplification of optical activity by enantioselective occlusion of amino acids by floating glycine crystals oriented at the air/water interface by hydrophobic additives. The system starts from an initial enantiomeric excess $L > D$ in solution. The horizontal arrows indicate the temporal sequence of events.

III. MATHEMATICAL MODEL

We transcribe the above reaction processes into the corresponding differential rate equations. Introduce concentration variables $a_r(t) = [A_r]$, $L_1(t) = [L_1]$, $D_1(t) = [D_1]$ and for the two host-plus-guest crystal orientations exposed towards the solution $f_{r,n}(t) = \{L_1 X_r D_n\}$ and $\bar{f}_{r,n}(t) = \{D_1 Y_r L_n\}$, respectively. We consider separately the kinetic equations for $f_{r,0}$, $f_{2,n}$, and then $f_{r,n}$ and similarly for the other enantiotopic face orientation. That is, we can treat the growth of pure host crystal, growth of guest on minimal host substrate and then the general *mixed* growth of both host and guest. Remember $f_{r,k} = f_{host,guest}$, so there must be a minimum host size r to accommodate the occluded guests.

Applying law of mass action we obtain the following kinetic equations:

$$\begin{aligned} \frac{da_1}{dt} = & -\mu_1 a_1 (L_1 + D_1) - 2\delta_{11} a_1^2 - \sum_{k=2}^{\infty} \delta_{1,k} a_1 a_k \\ & - a_1 \sum_r \sum_{n=0} \alpha_{r,n} (f_{r,n} + \bar{f}_{r,n}), \end{aligned} \quad (5)$$

$$\begin{aligned} \frac{da_r}{dt} = & -\mu_r a_r (L_1 + D_1) + \frac{1}{2} \sum_{k=1}^{r-1} \delta_{k,r-k} a_k a_{r-k} \\ & - \sum_{k=1}^{\infty} \delta_{r,k} a_r a_k, \quad (r \geq 2) \end{aligned} \quad (6)$$

$$\frac{dL_1}{dt} = -L_1 \sum_r \mu_r a_r - L_1 \sum_r \sum_{n=0} \xi_{r,n} \bar{f}_{r,n}, \quad (7)$$

$$\frac{dD_1}{dt} = -D_1 \sum_r \mu_r a_r - D_1 \sum_r \sum_{n=0} \xi_{r,n} f_{r,n}, \quad (8)$$

$$\begin{aligned} \frac{df_{r,0}}{dt} = & \mu_r L_1 a_r - \xi_{r,0} f_{r,0} D_1 \\ & + a_1 (\alpha_{r-1,0} f_{r-1,0} - \alpha_{r,0} f_{r,0}), \end{aligned} \quad (9)$$

$$\begin{aligned} \frac{d\bar{f}_{r,0}}{dt} = & \mu_r D_1 a_r - \xi_{r,0} \bar{f}_{r,0} L_1 \\ & + a_1 (\alpha_{r-1,0} \bar{f}_{r-1,0} - \alpha_{r,0} \bar{f}_{r,0}), \end{aligned} \quad (10)$$

$$\begin{aligned} \frac{df_{r,n}}{dt} = & D_1 (\xi_{r,n-1} f_{r,n-1} - \xi_{r,n} f_{r,n}) \\ & + a_1 (\alpha_{r-1,n} f_{r-1,n} - \alpha_{r,n} f_{r,n}), \quad (n \geq 1) \end{aligned} \quad (11)$$

$$\begin{aligned} \frac{d\bar{f}_{r,n}}{dt} = & L_1 (\xi_{r,n-1} \bar{f}_{r,n-1} - \xi_{r,n} \bar{f}_{r,n}) \\ & + a_1 (\alpha_{r-1,n} \bar{f}_{r-1,n} - \alpha_{r,n} \bar{f}_{r,n}), \quad (n \geq 1). \end{aligned} \quad (12)$$

For a closed system, we have the constant density constraint:

$$L_1 + D_1 + \sum_r r a_r + \sum_r \sum_n (r+n+1) (f_{r,n} + \bar{f}_{r,n}) = \text{const}. \quad (13)$$

The main problem with such a model is the large number of parameters that have been introduced: namely $\delta_{r,n}$, μ_r , $\alpha_{r,n}$ and $\xi_{r,n}$. It is thus clear we need to make several simplifications already at this stage.

A. Simplifications of the model

We assume that only the coalescence of two glycine monomers A_1 to form an A_2 dimer needs to be retained, and only A_2 dimer clusters are used to form new oriented host crystals when they encounter a hydrophobic amino acid monomer. We also assume that all rates are independent of cluster size, so that

$$\delta_{1,1} = \delta, \quad \delta_{r,k} = 0, \quad (\text{otherwise}) \quad (14)$$

$$\mu_2 = \mu, \quad \mu_r = 0, \quad (r = 1 \& r \geq 3) \quad (15)$$

$$\alpha_{r,n} = \alpha, \quad (r \geq 2), \quad \alpha_{1,n} = 0 \quad (16)$$

$$\xi_{r,n} = \xi, \quad (r \geq 2), \quad \xi_{1,n} = 0. \quad (17)$$

Then the above kinetic equations take the following form:

$$\frac{da_1}{dt} = -2\delta a_1^2 - \alpha a_1 \sum_{r=2} \sum_{n=0} (f_{r,n} + \bar{f}_{r,n}), \quad (18)$$

$$\frac{da_2}{dt} = \delta a_1^2 - \mu a_2 (L_1 + D_1), \quad (19)$$

$$\frac{dL_1}{dt} = -\mu L_1 a_2 - \xi L_1 \sum_{r=2} \sum_{n=0} \bar{f}_{r,n}, \quad (20)$$

$$\frac{dD_1}{dt} = -\mu D_1 a_2 - \xi D_1 \sum_{r=2} \sum_{n=0} f_{r,n}, \quad (21)$$

$$\frac{df_{2,0}}{dt} = \mu L_1 a_2 - (\xi D_1 + \alpha a_1) f_{2,0}, \quad (22)$$

$$\frac{d\bar{f}_{2,0}}{dt} = \mu D_1 a_2 - (\xi L_1 + \alpha a_1) \bar{f}_{2,0}, \quad (23)$$

$$\frac{df_{r,0}}{dt} = -\xi D_1 f_{r,0} + \alpha a_1 (f_{r-1,0} - f_{r,0}), \quad (r \geq 3) \quad (24)$$

$$\frac{d\bar{f}_{r,0}}{dt} = -\xi L_1 \bar{f}_{r,0} + \alpha a_1 (\bar{f}_{r-1,0} - \bar{f}_{r,0}), \quad (r \geq 3) \quad (25)$$

$$\frac{df_{2,n}}{dt} = \xi D_1 (f_{2,n-1} - f_{2,n}) - \alpha a_1 f_{2,n}, \quad (n \geq 1) \quad (26)$$

$$\frac{d\bar{f}_{2,n}}{dt} = \xi L_1 (\bar{f}_{2,n-1} - \bar{f}_{2,n}) - \alpha a_1 \bar{f}_{2,n}, \quad (n \geq 1) \quad (27)$$

$$\frac{df_{r,n}}{dt} = \xi D_1 (f_{r,n-1} - f_{r,n}) + \alpha a_1 (f_{r-1,n} - f_{r,n}), \quad (r \geq 3, n \geq 1) \quad (28)$$

$$\frac{d\bar{f}_{r,n}}{dt} = \xi L_1 (\bar{f}_{r,n-1} - \bar{f}_{r,n}) + \alpha a_1 (\bar{f}_{r-1,n} - \bar{f}_{r,n}), \quad (r \geq 3, n \geq 1). \quad (29)$$

As an important check on internal consistency, we verify explicitly that mass conservation holds. To this end, we consider the following change of variables

$$P = \sum_{r=3}^{\infty} f_{r,0}, \quad M_2 = \sum_{n=1}^{\infty} f_{2,n}, \quad M = \sum_{r=3}^{\infty} \sum_{n=1}^{\infty} f_{r,n}, \quad (30)$$

$$\bar{P} = \sum_{r=3}^{\infty} \bar{f}_{r,0}, \quad \bar{M}_2 = \sum_{n=1}^{\infty} \bar{f}_{2,n}, \quad \bar{M} = \sum_{r=3}^{\infty} \sum_{n=1}^{\infty} \bar{f}_{r,n}. \quad (31)$$

Then the above infinite collection of equations can be written in terms a mathematically closed set of just twelve equations:

$$\begin{aligned} \frac{da_1}{dt} &= -2\delta a_1^2 \\ &\quad -\alpha a_1 \left(f_{2,0} + M_2 + P + M + \bar{f}_{2,0} + \bar{P} + \bar{M} + \bar{M}_2 \right), \end{aligned} \quad (32)$$

$$\frac{da_2}{dt} = \delta a_1^2 - \mu a_2 (L_1 + D_1), \quad (33)$$

$$\frac{dL_1}{dt} = -\mu L_1 a_2 - \xi L_1 \left(\bar{f}_{2,0} + \bar{P} + \bar{M} + \bar{M}_2 \right), \quad (34)$$

$$\frac{dD_1}{dt} = -\mu D_1 a_2 - \xi D_1 \left(f_{2,0} + M_2 + P + M \right), \quad (35)$$

$$\frac{df_{2,0}}{dt} = \mu L_1 a_2 - (\xi D_1 + \alpha a_1) f_{2,0}, \quad (36)$$

$$\frac{d\bar{f}_{2,0}}{dt} = \mu D_1 a_2 - (\xi L_1 + \alpha a_1) \bar{f}_{2,0}, \quad (37)$$

$$\frac{dP}{dt} = -\xi D_1 P + \alpha a_1 f_{2,0}, \quad (38)$$

$$\frac{d\bar{P}}{dt} = -\xi L_1 \bar{P} + \alpha a_1 \bar{f}_{2,0}, \quad (39)$$

$$\frac{dM_2}{dt} = \xi D_1 f_{2,0} - \alpha a_1 M_2, \quad (40)$$

$$\frac{d\bar{M}_2}{dt} = \xi L_1 \bar{f}_{2,0} - \alpha a_1 \bar{M}_2, \quad (41)$$

$$\frac{dM}{dt} = \xi D_1 P + \alpha a_1 M_2, \quad (42)$$

$$\frac{d\bar{M}}{dt} = \xi L_1 \bar{P} + \alpha a_1 \bar{M}_2. \quad (43)$$

We need to have kinetic equations for the corresponding densities. The following definitions will accomplish this:

$$\rho_P = \sum_{r=3}^{\infty} (r+1) f_{r,0}, \quad (44)$$

$$\rho_{M_2} = \sum_{n=1}^{\infty} (n+3) f_{2,n}, \quad (45)$$

$$\rho_M = \sum_{r=3}^{\infty} \sum_{n=1}^{\infty} (r+n+1) f_{r,n}. \quad (46)$$

Then the kinetic equations for the densities follow:

$$\dot{\rho}_P = -\xi D_1 \rho_P + \alpha a_1 (4f_{2,0} + P), \quad (47)$$

$$\dot{\rho}_{M_2} = 4\xi D_1 f_{2,0} + \xi D_1 M_2 - \alpha a_1 \rho_{M_2}, \quad (48)$$

$$\dot{\rho}_M = \xi D_1 (P + \rho_P + M) + \alpha a_1 (\rho_{M_2} + M_2 + M). \quad (49)$$

There are of course analogous equations for the Z_2 or chiral partners $\bar{\rho}_P$, $\bar{\rho}_{M_2}$ and $\bar{\rho}_M$. To express the mass conservation in terms of these densities, define

$$\rho = 3f_{2,0} + \rho_{M_2} + \rho_P + \rho_M, \quad (50)$$

$$\bar{\rho} = 3\bar{f}_{2,0} + \bar{\rho}_{M_2} + \bar{\rho}_P + \bar{\rho}_M, \quad (51)$$

then the following constraint holds

$$a_1 + L_1 + D_1 + 2a_2 + \rho + \bar{\rho} = \text{const.} \quad (52)$$

This proves that total mass of the reactants is conserved in our scheme.

B. Linear Stability

It is useful at this stage to check if the model is actually capable of mirror symmetry breaking. Consider the following variables where H denotes pure host crystals, and M the mixed host plus guest crystals:

$$H = f_{2,0} + P, \quad (53)$$

$$\bar{H} = \bar{f}_{2,0} + \bar{P}, \quad (54)$$

$$M = M_2 + M, \quad (55)$$

$$\bar{M} = \bar{M}_2 + \bar{M}. \quad (56)$$

Then we can further reduce the system from twelve to only eight differential equations:

$$\frac{da_1}{dt} = -2\delta a_1^2 - \alpha a_1 (H + \bar{H} + M + \bar{M}), \quad (57)$$

$$\frac{da_2}{dt} = \delta a_1^2 - \mu a_2 (L_1 + D_1), \quad (58)$$

$$\frac{dL_1}{dt} = -\mu L_1 a_2 - \xi L_1 (\bar{H} + \bar{M}), \quad (59)$$

$$\frac{dD_1}{dt} = -\mu D_1 a_2 - \xi D_1 (H + M), \quad (60)$$

$$\frac{dH}{dt} = \mu L_1 a_2 - \xi D_1 H, \quad (61)$$

$$\frac{d\bar{H}}{dt} = \mu D_1 a_2 - \xi L_1 \bar{H}, \quad (62)$$

$$\frac{dM}{dt} = \xi D_1 H, \quad (63)$$

$$\frac{d\bar{M}}{dt} = \xi L_1 \bar{H}. \quad (64)$$

We can define three types of chiral polarizations η, θ, ϕ . Investigate mirror symmetry breaking by the change of variables:

$$\chi = L_1 + D_1, \quad w = H + \bar{H}, \quad z = M + \bar{M}, \quad (65)$$

$$\eta = \frac{L_1 - D_1}{\chi}, \quad \theta = \frac{H - \bar{H}}{w}, \quad \phi = \frac{M - \bar{M}}{z}. \quad (66)$$

The transformed equations Eqs.(57-64) read as follows:

$$\frac{da_1}{dt} = -2\delta a_1^2 - \alpha a_1 (w + z), \quad (67)$$

$$\frac{da_2}{dt} = \delta a_1^2 - \mu a_2 \chi, \quad (68)$$

$$\frac{d\chi}{dt} = -\mu a_2 \chi - \frac{\xi}{2} \chi (w(1 - \eta\theta) + z(1 - \eta\phi)), \quad (69)$$

$$\frac{d\eta}{dt} = \frac{\xi}{2} (1 - \eta^2) (w\theta + z\phi), \quad (70)$$

$$\frac{dw}{dt} = \mu a_2 \chi - \frac{\xi \chi w}{2} (1 - \eta\theta), \quad (71)$$

$$\frac{d\theta}{dt} = \frac{\mu a_2 \chi}{w} (\eta - \theta) + \frac{\xi \chi}{2} \eta (1 - \theta^2), \quad (72)$$

$$\frac{dz}{dt} = \frac{\xi \chi w}{2} (1 - \eta\theta), \quad (73)$$

$$\frac{d\phi}{dt} = \frac{\xi \chi w}{2z} (\theta - \eta) - \frac{\xi \chi w}{2z} \phi (1 - \eta\theta). \quad (74)$$

Consider the stability of the symmetric solution $\eta = \theta = \phi = 0$. Linearize the system of the three corresponding rate equations and determine stability of the solution from the Jacobian matrix:

$$\begin{pmatrix} 0 & \frac{\xi}{2}w & \frac{\xi z}{2} \\ \frac{\mu a_2 \chi}{w} + \frac{\xi \chi}{2} & -\frac{\mu a_2 \chi}{w} & 0 \\ -\frac{\xi}{2z}\chi w & \frac{\xi}{2z}\chi w & -\frac{\xi}{2z}\chi w \end{pmatrix}. \quad (75)$$

Expansion along the minors yields the determinant \det which is also given by the product of the three eigenvalues λ_i :

$$\det = +\frac{\xi^2}{4z}\chi^2 w^2 \left(\frac{\mu a_2}{w} + \frac{\xi}{2} \right) + \frac{\xi^3 \chi^2 w}{8} = \prod_{i=1}^3 \lambda_i > 0. \quad (76)$$

This result immediately tells us that the symmetric or racemic state is *unstable*. To confirm this, first consider the case where all three eigenvalues λ_i are real. Then the only way for their product to be positive is if the individual eigenvalues have the algebraic signs $(+, +, +)$, or $(+, -, -)$ (the order is not important): the point is, either one eigenvalue or else all three must be positive, and thus in both cases the *symmetric state is unstable*. So chiral symmetry will be broken in this infinite but closed model. Note that the remaining sign possibilities $(-, -, -)$ and $(+, +, -)$ (again, the order is not important) would yield instead a negative determinant $\det < 0$, and could imply stable or unstable, respectively. This latter situation is inconclusive without further analysis. If on the other hand \det has complex eigenvalues, these always occur in complex conjugate pairs, and without loss of generality we may suppose that $\lambda_3 = \lambda_2^*$. Then $\det = \lambda_1 |\lambda_2|^2 > 0$ if and only if $\lambda_1 > 0$, and again we conclude that the symmetric state is unstable. The expression for \det depends on the rate of enantioselective occlusion ξ and the rate for hydrophobic orientation of host crystals μ and suggests that the former is more important than the latter for driving the symmetry breaking: this is so because we can set $\mu = 0$ in Eq. (76) and $\det > 0$ remains positive, so the racemic state remains unstable. But if we set $\xi = 0$, then \det vanishes identically and the result is inconclusive at this lowest order. On the other hand, we note that neither the rate of glycine up-take α nor the rate of glycine cluster formation δ appear explicitly in the determinant, suggesting that these processes in and of themselves are *not* the decisive factors for symmetry breaking. These expectations are in accord with the processes depicted in the scheme represented in Fig. 1: the crucial amplification cycle involves the orientation and occlusion steps only. The processes of glycine aggregation in solution (δ) and growth by glycine up-take (α) are *prior* events that are not involved in this cycle. Thus, at this stage, we may be confident that our model will qualitatively capture the main symmetry breaking aspects of the actual experiment, and that the bare minimal ingredients required for this are crystal orientation and enantioselective occlusion.

The above model allows unlimited growth of the mixed host plus guest crystals. A severe *truncation* yielding a minimal model consists of an $r = 2$ glycine host with at most one occluded amino acid guest $n = 1$ per host. The determinant in this case is given by Eq.(76) after deleting the $\xi^3 \chi^2 w/8$ term. The linear stability analysis carried out for this truncated model leads to the same conclusions as above. We thus find that the symmetric state is unstable in two opposite limiting cases of the underlying model: for glycine host dimers and one occluded guest as well as for arbitrarily large glycine host crystals $r < \infty$ accommodating an unlimited number $n < \infty$ of occluded guests. Thus we may expect that the symmetric state will be unstable for all intermediate host/guest truncations of the model. This expectation is confirmed by the numerical simulations presented below.

IV. COMPLETE TRUNCATED MODEL

The model leads to the unlimited growth of both the glycine host crystals as well as to an unlimited number of enantiomers that can be occluded per host crystal. The experiments by contrast yield finite size mixed glycine plus host crystals with a rather uniform size distribution and with each host occluding a small percentage of the available amino acids[5, 6]. We must also recognize the fundamental physical limitation imposed by the fact that the air/water interface is of finite area: the experiments are carried out in a bounded reaction domain which means only a finite air/water interface is available for the crucial orientation/amplification processes to take place. We will thus need to model the effect of a bounded (finite area) interface. Once the interface is *covered* by floating glycine crystals, no more hydrophobic amino acids can diffuse up to the surface, the remaining reactions from this point on can only be the glycine up-take from the solution and the enantioselective occlusion of the amino acids in solution. The finite size of the experiment implies that these latter two processes must be limited as well; we will thus consider how to truncate both the host growth as well as the number of occluded guests per host. The reactions will thus stop at some point: there must be maximum values of both R and N such that $2 \leq r \leq R$ and hosts $0 \leq n \leq N(R)$. Each instantaneous size r of the host crystal will be allowed to occlude up to maximum number $n(r)$ of guests. We can account for all

of these limiting features by implementing certain truncations or cut-offs that we apply to the underlying model. At the same time, we complete the model by including the kinetic inhibition effect.

A. Hydrophobic and kinetic effects and hydrophobic and hydrophilic additives

The experiment demonstrates that the glycine crystals at the interface are oriented via two distinct effects: (i) hydrophobic and (ii) kinetic. The former is due to the induction by hydrophobic amino acids while the latter is achieved through the inhibition of nucleation and growth of the oriented crystals. The hydrophobic effect is confined to hydrophobic amino acids but the kinetic effect applies to all α -amino acid *additives*, both hydrophobic and hydrophilic. It is important to bear in mind that there is hence not a one-to-one correspondence between effects and additives. For this reason, in the full model below, we introduce the two kinds of additives and talk about the effect of the additives rather than the hydrophobic or kinetic effects *per se*, since the latter are not easily separable. The two effects however do act in the same direction. The inclusion of both types of additive leads to only a minor modification and leads to a complete model. We also implement a consistent truncation where R is maximum size of the glycine host crystal and $n = n(r)$ is a maximum number of occluded amino acid guest monomers for any instantaneous host size r .

For completeness, we list the full set of chemical reactions defining the final model. Formation of glycine crystals/clusters in solution.



Diffusion of amino acids in bulk solution to interface implying nucleation of *oriented* glycine crystals at the air/water interface in presence of hydrophobic *LD*-amino acids.



The effective conversion rate of bulk amino acids to amino acids at the interface will depend on a critical glycine crystal interface concentration f_c . Beyond this concentration, no more hydrophobic amino acids will diffuse up to the surface, and consequently no more fresh glycine crystals can nucleate at the surface. To implement this we will take

$$\mu(f_c) = \mu_0 \Theta(f_c - f(t)), \quad (79)$$

where $f(t)$ is be the instantaneous concentration of glycine crystals, with and without occluded amino acids, at time t , and f_c is a critical surface concentration which is supposed to effectively mock the finite interface. Here:

$$\mu(t) = \mu_0 \Theta\left(f_c - \sum_{r=3}^R \sum_{n=0}^{\Gamma} (f_{r,n}(t) + \bar{f}_{r,n}(t))\right), \quad (80)$$

where the unit step function is defined as

$$\Theta(x) = \begin{cases} 1, & x > 0 \\ 0, & x < 0. \end{cases} \quad (81)$$

Once the instantaneous concentration of glycine crystals reaches f_c then this reaction shuts off, from which point on the hydrophobic orienting effect ceases to act. This is an effective way of implementing the finite interface area constraint without adding complicated spatial dependence to the model.

In keeping with the above remarks and experimental facts, we must allow for the hydrophobic amino acids to inhibit those glycine nuclei exposing their enantiotopic faces towards the solution from further growth. We also introduce a second species of hydrophilic amino acids \bar{L}, \bar{D} , which can only participate in the kinetic effect.

Inhibition of the fresh glycine seeds by kinetic effect due to the *hydrophobic* additives.



Inhibition of the fresh glycine seeds by kinetic effect due to the *hydrophilic* additives:

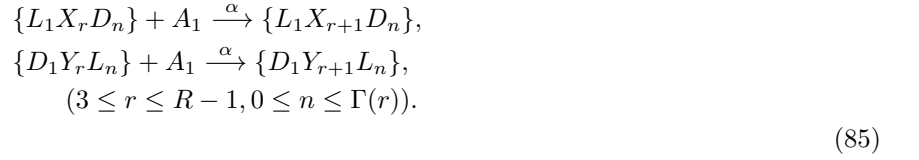


the total inert product of this inhibited crystal seeds (via either the hydrophobic or hydrophilic additives) will be denoted as $P(t)$. An excess of $L > D$ in solution inhibits glycine nuclei exposing their $(0\bar{1}0)$ towards solution[4], preventing their further growth, and analogously for $D > L$. We have opted to model this as a cross-inhibition reaction, in the spirit of the Frank model, except here we form a small tetramer unit with a glycine dimer trapped between the hydrophobic templatator and the hydrophilic growth inhibitor. The templatator and growth inhibitor have opposite handedness. So, if the glycine host crystal occludes an amino acid having the opposite chirality of the nucleator amino and located on the opposite enantiotopic face, then the seed glycine crystal has been inhibited and can not grow further. Otherwise, if the seed grows by incorporating a glycine monomer, it can escape this “bottleneck”, and will continue to grow via glycine up-take or by amino acid occlusion.

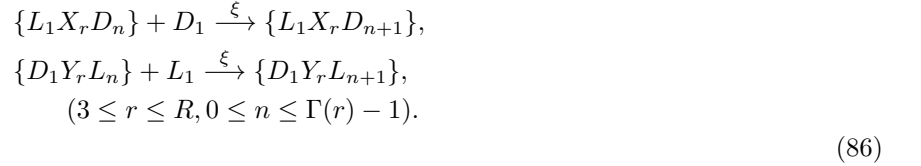
The remainder of the reactions are unchanged, except that now we impose the finite size truncations (bounds on r and on n) remarked above. Growth of the oriented fresh glycine hosts.



Growth of the oriented host glycine crystal.



Enantioselective occlusion of the amino acid monomers from solution.



Each host glycine crystal can grow by incorporating achiral glycine monomers from the solution, so we must impose a maximum number R of glycine monomers forming the host crystal. By the same token, we impose a maximum number of guest chiral monomers N to be occluded in the host crystal. The maximum number of guests that a crystal can occlude depends on the number of host monomers of the crystal, so we define $\Gamma(r) = \text{Floor}[\gamma r]$, where $\text{Floor}[\gamma r]$ rounds the elements of γr to the nearest integer less than or equal to γr and $0 < \gamma \leq 1$ is a free parameter that allows us to vary the percentage of occluded amino acids.

With these truncations and limits and for both types of additives, the final set of kinetic equations reads as follows:

$$\begin{aligned} \frac{da_1}{dt} &= -2\delta a_1^2 \\ &\quad -\alpha a_1(f_{2,0} + \bar{f}_{2,0} + \sum_{r=3}^{R-1} \sum_{n=0}^{\Gamma(r)} (f_{r,n} + \bar{f}_{r,n})), \end{aligned} \quad (87)$$

$$\frac{da_2}{dt} = \delta a_1^2 - \mu a_2(L_1 + D_1), \quad (88)$$

$$\frac{dL_1}{dt} = -\mu L_1 a_2 - \xi L_1(\bar{f}_{2,0} + \sum_{r=3}^R \sum_{n=0}^{\Gamma(r)-1} \bar{f}_{r,n}), \quad (89)$$

$$\frac{dD_1}{dt} = -\mu D_1 a_2 - \xi D_1(f_{2,0} + \sum_{r=3}^R \sum_{n=0}^{\Gamma(r)-1} f_{r,n}), \quad (90)$$

$$\frac{d\bar{L}_1}{dt} = -\beta \bar{f}_{2,0} \bar{L}_1, \quad (91)$$

$$\frac{d\bar{D}_1}{dt} = -\beta f_{2,0} \bar{R}_1, \quad (92)$$

$$\frac{dP}{dt} = \xi(D_1 f_{2,0} + L_1 \bar{f}_{2,0}) + \beta(\bar{D}_1 f_{2,0} + \bar{L}_1 \bar{f}_{2,0}), \quad (93)$$

$$\begin{aligned} \frac{df_{r,n}}{dt} &= A(r,n)\mu L_1 a_2 + B(r,n)\xi D_1 f_{r,n-1} - C(r,n)\xi D_1 f_{r,n} \\ &\quad + D(r,n)\alpha a_1 f_{r-1,n} - E(r,n)\alpha a_1 f_{r,n} - F(r,n)\beta \bar{D}_1 f_{r,n}, \\ &\quad (2 \leq r \leq R, 0 \leq n \leq \Gamma(r)) \end{aligned} \quad (94)$$

$$\begin{aligned} \frac{d\bar{f}_{r,n}}{dt} &= A(r,n)\mu D_1 a_2 + B(r,n)\xi L_1 \bar{f}_{r,n-1} - C(r,n)\xi L_1 \bar{f}_{r,n} \\ &\quad + D(r,n)\alpha a_1 \bar{f}_{r-1,n} - E(r,n)\alpha a_1 \bar{f}_{r,n} - F(r,n)\beta \bar{L}_1 \bar{f}_{r,n} \\ &\quad (2 \leq r \leq R, 0 \leq n \leq \Gamma(r)). \end{aligned} \quad (95)$$

For a more streamlined presentation as well as for simulation purposes we prefer to write an single differential equation for the $f_{r,n}$ and another one for the $\bar{f}_{r,n}$, whose individual terms are switched on or off depending on the values of r, n . To this end, we have defined the following *switch* functions A, B, C, D, E and F :

$$\begin{aligned} A(r,n) &= 1 \quad \text{if } r = 2 \& n = 0 \\ B(r,n) &= 1 \quad \text{if } r \geq 3 \& n \geq 1 \\ C(r,n) &= 1 \quad \text{if } (r = 2 \& n = 0) \vee \\ &\quad (r \geq 3 \quad \& \quad n \leq \Gamma(r) - 1) \end{aligned} \quad (96)$$

$$\begin{aligned} D(r,n) &= 1 \quad \text{if } (r \geq 3 \& n \leq \Gamma(r) - 1) \\ E(r,n) &= 1 \quad \text{if } (r = 2 \& n = 0) \vee \\ &\quad (3 \leq r \leq R - 1) \end{aligned} \quad (97)$$

$$F(r,n) = 1 \quad \text{if } r = 2 \& n = 0 \quad (98)$$

The above set of kinetic equations satisfy the constant density constraint which we monitor and verify in all the numerical simulations:

$$\begin{aligned} &L_1 + D_1 + \bar{L}_1 + \bar{D}_1 + 4P \\ &+ a_1 + 2a_2 + \sum_{r=2}^R \sum_{n=0}^{\Gamma(r)} (r+n+1)(f_{r,n} + \bar{f}_{r,n}) = \text{const}. \end{aligned} \quad (99)$$

V. NUMERICAL RESULTS

We are interested in testing out the effectiveness of the proposed orientation and amplification cycle (Figure 1) as this is actually represented in the model. At the same time, we can also control the amounts of each type of additive and assess the relative importance of the two orienting effects, namely hydrophobic and kinetic. The results are quantified and presented in terms of a number of experimentally relevant chiral measures. The percent enantiomeric excess of the hydrophobic additives in solution is

$$ee(\%) = \frac{[L_1] - [D_1]}{[L_1] + [D_1]} \times 100. \quad (100)$$

When hydrophilic amino acids are added, a corresponding percent enantiomeric excess can also be defined:

$$ee_h(\%) = \frac{[\bar{L}_1] - [\bar{D}_1]}{[\bar{L}_1] + [\bar{D}_1]} \times 100. \quad (101)$$

We consider the percent excess of the occluded amino acids via

$$ee_{occlude}(\%) = \frac{L_{occluded} - D_{occluded}}{L_{occluded} + D_{occluded}} \times 100. \quad (102)$$

In keeping with the experimental reports, this counts the amino acids occluded in the host crystal enantiotopic faces exposed to the solution. An important aspect of the experiment is the degree of crystal orientation at the interface. The following parameter measures the orientation degree of the crystals at the interface:

$$od(\%) = \frac{f - \bar{f}}{f + \bar{f}} \times 100. \quad (103)$$

and gives us a direct measure of the orientation. Here f and \bar{f} are the total amount of crystal of each type (i.e., pyramids and plates[6]) at the surface (omitting the floating inhibited seeds):

$$f = \sum_{r=3}^R \sum_{n=0}^{\Gamma(r)} f_{r,n} \quad \bar{f} = \sum_{r=3}^R \sum_{n=0}^{\Gamma(r)} \bar{f}_{r,n}$$

The differential rate equations Eqs. (87-95) were numerically integrated using the version 7 Mathematica program package. The results were monitored to verify that the total system mass Eq. (99) remained constant in time. We organize and present our main results in terms of the types of additives employed, that is, hydrophobic and/or hydrophilic amino acids.

A. Hydrophobic additives

To simulate the following cases, only hydrophobic additives have been added to the saturated glycine solution. So we maintain zero concentration of the hydrophilic additives $[L_1]_0 = [D_1]_0 = 0$ throughout the following sequence of simulations. All the numerical results have been obtained for the values $R = 50$, $\gamma = 0.1$, $\alpha = 10^{-3}$, $\delta = 10^{-6}$, $\xi = 1$, $\mu_0 = 10^{-6}$ and $f_c = 0.01M$. We provide some brief rationale for these selected values. The experiment reports that only a small fraction of the α -amino acids (0.02 – 0.2%) is subsequently occluded into the bulk of the growing glycine crystals. We therefore try to maximize the host crystal size R so as to be able to achieve small fractions of occluded guests. Computational limitations (memory and time) forced us to compromise and we thus choose $R=50$ and $\gamma = 0.1$ (for the desired values $\gamma = 0.0002 - 0.002$, the corresponding R is so great as to exceed available computational resources). Next, we aimed to reproduce as closely as possible the reported details concerning the growth of crystals at the air/solution interface. The first step was to find reactions rates satisfying these conditions, as is shown in our Table 1. Since we do not have spatial information (and thus can not distinguish between pyramids and plates), we tried to find the reaction rates (at least the relation between them) reproducing this behaviour (supposing that pure platforms were the pyramids and the product of the inhibition yields the plates). This strategy led us to employ the values of α, δ, ξ and μ given above.

We have used the same glycine concentrations as reported in the experiments[6]. Thus, in a typical experiment 10 g of glycine ($m_{gly} = 10g$) were dissolved in 30 ml ($Vol = 0.03l$) of double distilled water, where its molar mass $Mm_{gly} = 75.07g \cdot mol^{-1}$. Following this, the initial glycine concentration should therefore be $[a_1]_0 = m_{gly}/(Mm_{gly} \times$

$Vol) = 4.44 \text{ mol} \cdot \text{l}^{-1}$, and this is the value of initial glycine monomer concentration used in all the simulations reported here. For the glycine dimers we initially set $[a_2]_0 = 0$, and zero initial concentrations of the oriented glycine crystals at the interface: $(f_{r,n})_0 = 0$ and $(\bar{f}_{r,n})_0 = 0$, respectively. Finally, from the initial enantiomeric excess ee_0 and the relative weight of additive to glycine, (w/w_{gly}) , we can deduce the initial concentrations $[L]_0$ and $[D]_0$ straightforwardly from the pair of Eqs. (104).

$$\begin{aligned} [L]_0 &= \frac{(w/w_{gly})m_{gly}(1+ee_0)}{2Mm_{gly} \times Vol}, \\ [D]_0 &= \frac{(w/w_{gly})m_{gly}(1-ee_0)}{2Mm_{gly} \times Vol}. \end{aligned} \quad (104)$$

We ignore the molar mass differences Mm between glycine and the α -amino acid molar masses ($Mm(Ala) = 89.09 \text{ gmol}^{-1}$, $Mm(Leu) = 131.17 \text{ gmol}^{-1}$, $Mm(Val) = 117.15 \text{ gmol}^{-1}$, $Mm(Val) = 105.09 \text{ gmol}^{-1}$).

1. Racemic mixtures of hydrophobic additives

. In this case, the composition of the complete solution is obtained by adding a racemic hydrophobic additive to the supersaturated solution of glycine. This means we start with zero initial excess of chiral hydrophobic monomers: $ee_0 = 0$. We want to observe the effect of varying the relative mass of the chiral monomers with respect to the amount of glycine (w/w_{gly}) . The numerical results obtained in these simulations are shown in Table I. For each relative initial concentration of additives (w/w_{gly}) we evaluate the total concentration $f + \bar{f}$ of the oriented mixed host plus guest crystals at the interface summed over both orientations, and P , the total concentration of nuclei or seed crystals killed by the kinetic inhibition effect and their associated chiral polarizations or excesses. Recall that *both* the hydrophobic and kinetic effects are operative for hydrophobic amino acid additives.

As we see in Table I, for all cases the interface is covered with crystals of both orientations. This is not surprising, since we start from a racemic composition, but no initial ‘‘Adam’’ crystal, this must lead to an equal ratio $f : \bar{f} = 1 : 1$ of the enantiotopic faces exposed to the solution, thus $od(\%) = 0$. By the same token, the ee of the solution and the net ee_{oc} of occluded monomers must also be zero. There is no symmetry breaking in this idealized situation. In the actual experiments, floating glycine crystals can exhibit two distinct morphologies, either pyramidal or plates [5, 6]. The former are the result of the hydrophobic orienting effect, while the latter morphology results from the kinetic inhibition effect. Because of this, we can infer the crystal morphologies implicit in our simulations: indeed, the concentrations f and \bar{f} correspond to the pyramidal form (resulting from the hydrophobic effect) whereas the concentration P corresponds to the plate-like form (resulting from the kinetic effect).

Thus for values of w/w_{gly} as low as 10^{-4} , we found enantiomorphous pyramids showing thus no macroscopic evidence for the kinetic retardation of growth by for example, leucine. By increasing the additive concentration, a *morphological change* of the floating glycine crystals is numerically observed, from pyramids $f + \bar{f}$ to plates P (inhibited seeds). The concentration of the pyramids decreases while that of the plates increases as we increase the concentration of the racemic additive. This simulation result is in qualitative accord with the experiment where an evident morphological change from pyramids to plates was observed upon increasing the leucine concentration (i.e., the hydrophobic additive employed there). [6]. The initially racemic amino acid solution remains racemic at all later times, no matter how large the initial amount of additives is.

TABLE I: Orientation of floating glycine crystals in the presence of mixtures of (L,D) hydrophobic additives

| (L,D) | | | | | |
|-------------|----------------------------------|----------------------------------|------|------|-----------|
| Hydrophobic | $f + \bar{f}$ | P | od | ee | ee_{oc} |
| w/w_{gly} | $\text{mol} \cdot \text{l}^{-1}$ | $\text{mol} \cdot \text{l}^{-1}$ | (%) | (%) | (%) |
| 10^{-4} | $8.15 \cdot 10^{-5}$ | $4.38 \cdot 10^{-6}$ | 0 | 0 | 0 |
| 10^{-3} | $6.33 \cdot 10^{-4}$ | $3.54 \cdot 10^{-4}$ | 0 | 0 | 0 |
| 10^{-2} | $2.38 \cdot 10^{-3}$ | $1.51 \cdot 10^{-2}$ | 0 | 0 | 0 |
| 10^{-1} | $3.48 \cdot 10^{-3}$ | $2.12 \cdot 10^{-1}$ | 0 | 0 | 0 |

2. Racemic mixture hydrophobic additives + an initial oriented glycine crystal

The reaction scheme in Figure 1 starts from a *first random crystallization*, so we include this feature in the initial conditions. We consider the previous situation ($ee_0 = 0$) and suppose that there is one single crystal of glycine exposing say the (010) face toward the solution at an initial time; this means starting with a small initial concentration of $(f_{2,0})_0$. Since only one initial crystal can not be taken, it can however be "modeled" taking by a fraction of the critical interface concentration f_c of glycine crystals: $(f_{2,0})_0 = x f_c$, where $x \ll 1$ is given in the first column of Table II. There we display the numerical results for this particular situation, starting from an initial concentration of (LD)-hydrophobic amino acids $w/w_{gly} = 0.01$. The simulation results show a preferential (010) orientation of the glycine crystals at the surface induced by the initial (010) crystal. Even if this preferential orientation is not exclusive $od < 100\%$, an optically active solution is still generated, $ee = 100\%$.

The single crystal occludes the *D* enantiomers enantioselectively, thus enriching the aqueous solution with the *L* monomers. If this small excess can induce preferential orientation of the further growing crystals of glycine again with the (010) face pointing toward the solution, replication will ensue by cascade mechanism finally leading to a separation of enantiomeric territories[6]. From Table II we see that increasing the initial concentrations of the first oriented Adam crystals leads to increased degree of orientation od , and to increased enantiomeric excesses of both the amino acids in solution ee and of those that have been occluded by the pyramidal crystals, ee_{oc} . Dynamical aspects of the symmetry breaking can be appreciated from the time evolution of the concentrations and chiral excesses as displayed in Figure 3.

TABLE II: Orientation of floating glycine crystals in the presence of mixtures of (L,D) hydrophobic additives and "one" initial oriented crystal

| $(f_{2,0})_0/f_c$ | $f + \bar{f}$ | P | od | ee | ee_{oc} |
|-------------------|----------------------|----------------------|-------|------|-----------|
| x | $mol \cdot l^{-1}$ | $mol \cdot l^{-1}$ | (%) | (%) | (%) |
| 0.01 | $3.02 \cdot 10^{-3}$ | $1.51 \cdot 10^{-2}$ | 30.04 | 100 | 7.10 |
| 0.05 | $4.59 \cdot 10^{-3}$ | $1.47 \cdot 10^{-2}$ | 62.46 | 100 | 21.55 |
| 0.1 | $6.11 \cdot 10^{-3}$ | $1.42 \cdot 10^{-2}$ | 76.32 | 100 | 33.60 |

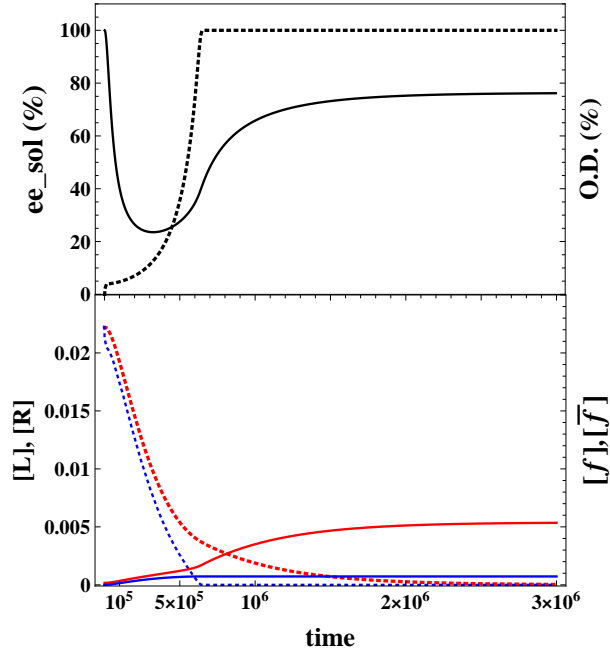


FIG. 3: Racemic mixture hydrophobic additives + an initial oriented glycine crystal. Initial conditions: $ee_0 = 0$, $w/w_{gly} = 0.01$, $[f_{2,0}]_0 = 10^{-3} f_c$, $ee_h = 0$, and $w_h/w_{gly} = 0$. Upper figure: dotted line represents the enantiomeric excess ee of solution and the solid line the orientation degree od . Lower figure: the dotted lines represent the concentrations of the hydrophobic enantiomers (where $[L]$ is the upper dotted curve), the solid lines represent the total concentration of oriented crystals (where $[f]$ is the upper solid curve).

3. Chiral hydrophobic additives

Instead of racemic hydrophobic additives we next consider adding a chiral hydrophobic compound (i.e., L- α -amino acids) to the supersaturated solution of glycine. This means we now start with an initial excess of the chiral hydrophobic monomers in solution so that $ee_0 = 1$. Table III shows the results for different concentrations in terms of the quoted w/w_{gly} values. As expected, in the presence of a resolved hydrophobic α -amino acid, the system achieves exclusive orientation at the interface: $od = 100\%$ and the excess ee of the remaining amino acids in solution is 100%. In this situation, there can be no amino acids occluded by the oriented crystals at the interface since the system lacks the D -monomer, hence ee_{oc} is not defined. Moreover without D monomers, the kinetic effect is inoperative and so $P = 0$: no plates can be formed, only pyramidal crystals. When L- α -amino acids are used, these pyramids are exclusively (010) oriented (the face exposed towards the solution). By symmetry, D amino acids would induce the enantiomorphous (0 $\bar{1}$ 0) oriented pyramids[6].

TABLE III: Orientation of floating glycine crystals induced by resolved L-hydrophobic additives (See Table III)[6]

| (L) | | | | | |
|-------------|----------------------|--------------------|------|------|-----------|
| Hydrophobic | $f + \bar{f}$ | P | od | ee | ee_{oc} |
| w/w_{gly} | $mol \cdot l^{-1}$ | $mol \cdot l^{-1}$ | (%) | (%) | (%) |
| 0.01 | 10^{-2} | 0 | 100 | 100 | - |
| 0.05 | 10^{-2} | 0 | 100 | 100 | - |
| 0.1 | $1.01 \cdot 10^{-2}$ | 0 | 100 | 100 | - |
| 0.5 | $1.02 \cdot 10^{-2}$ | 0 | 100 | 100 | - |

B. Hydrophilic additives

We now treat the general situation where both hydrophobic and hydrophilic additives are added to the supersaturated glycine solution. The following numerical results have been obtained for the values $R = 50$, $\gamma = 0.1$, $\alpha = 10^{-3}$, $\delta = 10^{-6}$, $\beta = \xi = 1$, $\mu_0 = 10^{-6}$ and $f_c = 0.01M$. As before, the initial glycine monomer concentration is $[a_1]_0 = 4.44 mol l^{-1}$ and for the initial glycine dimer concentration we set $[a_2]_0 = 0$ and zero initial concentrations of the oriented glycine crystals at the interface: $(f_{r,n})_0 = 0$, $(\bar{f}_{r,n})_0 = 0$. Controlling the amount of hydrophilic additives gives us an independent control of the kinetic inhibition effect.

1. Racemic mixtures of hydrophilic additives

The complete amino acid solution is now composed of a mixture of both *racemic* hydrophobic α -amino acids and by *racemic* hydrophilic α -amino acids. Here, the role of the hydrophobic additive is only to induce oriented crystallization at the air/water interface. Since its composition is racemic, this leads to an equal ratio $f : \bar{f} = 1 : 1$ of enantiotopic faces exposed to the solution, and for this we use a concentration corresponding to $w/w_{gly} = 0.01$. Thus the corresponding initial excesses of chiral hydrophobic and hydrophilic monomers are $ee_0 = 0$ and $ee_{h0} = 0$, respectively. There is no initial Adam crystal. We then observe what effect, if any, varying the amount of the hydrophilic additives has on this initial orientation.

Numerical results showing the effect of varying the relative mass of hydrophilic chiral monomers (w/w_{gly}) are shown in Table IV. No matter how large the amount of hydrophilic monomers, in the presence of racemic additives of both types, the surface is still covered with crystals of both orientations which immediately implies that the net excess of occluded monomers is zero. Note the solution achieves an extremely feeble optical activity. In fact, these excesses are only slightly greater or at the same level as the enantiomeric excess expected from pure statistical fluctuations[13]. Just as reported in the experiment, we observe how the amount of plates is much greater than the amount of enantiomorphous pyramids: $P > (f + \bar{f})$ [6].

TABLE IV: Orientation of floating glycine crystals in the presence of racemic mixtures of hydrophilic additives and 1% hydrophobic (L,D) amino acids

| (L,D) | | | | | |
|-------------|----------------------|----------------------|------|------------------|-----------|
| Hydrophilic | $f + \bar{f}$ | P | od | ee | ee_{oc} |
| w/w_{gly} | $mol \cdot l^{-1}$ | $mol \cdot l^{-1}$ | (%) | (%) | (%) |
| 0 | $2.38 \cdot 10^{-3}$ | $1.51 \cdot 10^{-2}$ | 0 | 0 | 0 |
| 0.01 | $1.08 \cdot 10^{-3}$ | $2.86 \cdot 10^{-2}$ | 0 | $0 \sim 10^{-8}$ | 0 |
| 0.05 | $3.44 \cdot 10^{-4}$ | $3.89 \cdot 10^{-2}$ | 0 | $\sim 10^{-7}$ | 0 |
| 0.1 | $1.86 \cdot 10^{-4}$ | $4.14 \cdot 10^{-2}$ | 0 | $\sim 10^{-5}$ | 0 |
| 0.5 | $3.99 \cdot 10^{-5}$ | $4.38 \cdot 10^{-2}$ | 0 | $\sim 10^{-7}$ | 0 |

2. Chiral hydrophilic additive

Just as in the previous simulation, the amino acid solution is composed of a racemic mixture of hydrophobic α -amino acids merely to induce the $X : Y = 1 : 1$ crystallization at the air/water interface and again we use $w/w_{gly} = 0.01$. But this time, we add *chiral* hydrophilic additives, and without loss of generality we take the *L* enantiomer. This is then a situation described by the initial excesses of hydrophobic and hydrophilic monomers given by $ee_0 = 0$ and $eeh_0 = 1$, respectively. Here, we are interested in the effect of varying the relative mass of hydrophilic chiral monomers (w/w_{gly}). Table V presents the numerical results for this situation. As we can see there, the presence of a chiral hydrophilic additive induces a preferential orientation, it is an indirect mechanism, since the kinetic effect inhibits the growth of the crystal nuclei that would otherwise expose the *Y*-face towards solution. Even if the orientation is not exclusive but only preferential, the solution does become optically active for low concentrations of the hydrophilic additive. And from the Table we see that territorial separation of the enantiomers is achieved.

TABLE V: Orientation by kinetic effect of floating glycine crystals in the presence of resolved hydrophilic additives and 1% hydrophobic (L,D)

| (L) | | | | | |
|-------------|----------------------|----------------------|-------|------|-----------|
| Hydrophilic | $f + \bar{f}$ | P | od | ee | ee_{oc} |
| w/w_{gly} | $mol \cdot l^{-1}$ | $mol \cdot l^{-1}$ | (%) | (%) | (%) |
| 0 | $2.38 \cdot 10^{-3}$ | $1.51 \cdot 10^{-2}$ | 0 | 0 | 0 |
| 10^{-6} | $2.38 \cdot 10^{-3}$ | $1.51 \cdot 10^{-2}$ | 0.51 | 100 | 0.08 |
| 10^{-5} | $2.51 \cdot 10^{-3}$ | $1.51 \cdot 10^{-2}$ | 8.43 | 100 | 1.56 |
| 10^{-4} | $3.28 \cdot 10^{-3}$ | $1.52 \cdot 10^{-2}$ | 38.88 | 100 | 9.21 |
| 10^{-3} | $6.10 \cdot 10^{-3}$ | $1.52 \cdot 10^{-2}$ | 79.03 | 100 | 33.36 |
| 10^{-2} | $1.00 \cdot 10^{-2}$ | $1.51 \cdot 10^{-2}$ | 96.26 | 100 | 76.09 |
| 10^{-1} | $1.00 \cdot 10^{-2}$ | $1.51 \cdot 10^{-2}$ | 99.51 | 100 | 96.60 |

The hydrophilic additives have an indirect orienting effect upon the floating glycine crystals in that they inhibit or kill the glycine nuclei so that these are unable to occlude. Only the hydrophobic additives can directly induce orientation. A typical time evolution of the symmetry breaking in this situation is depicted in Figure 4.

3. Hydrophobic vs. Hydrophilic additives

Next we study how hydrophobic and hydrophilic additives of *opposite* chiralities compete to induce a preferential orientation of the glycine crystals at the interface. To emphasize this competition, the amino acid solution will be composed of strictly (L)-hydrophobic and (D)-hydrophilic α -amino acids. So, initially we have $ee_0 = 1$, $eeh_0 = -1$. Take the (L) hydrophobic additive concentration to be $w/w_{gly} = 0.01$, and we vary the (D) hydrophilic additive concentration. Table VI shows there is a clear ability of the resolved hydrophobic α -amino acids to induce a specific orientation of the floating glycine crystals, even in the presence of large excesses of the hydrophilic α -amino acids of the opposite absolute configuration[6]. This can be compared with Table IV[6], which established experimentally the

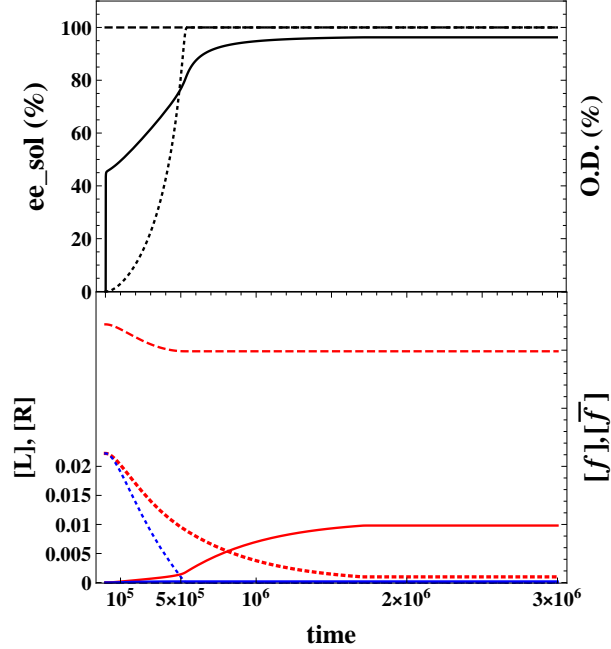


FIG. 4: Chiral hydrophilic additive. Initial conditions: $ee_0 = 0$, $w/w_{gly} = 0.01$, $ee_h0 = 1$, $w_h/w_{gly} = 0.01$. Upper figure: the dotted line represents the enantiomeric excess ee of the hydrophobic additives in solution, the solid line the orientation degree od , and the dashed line is the ee_h of the hydrophilic additive. Lower figure: dotted lines represent the concentrations of the hydrophobic additives (where $[L]$ is the upper dotted curve), the solid lines represent the total amount of oriented crystals of each type ($[f]$ is the upper solid curve), and dashed line represents the hydrophilic monomer concentration: $[\bar{L}]$.

dominance of the hydrophobic effect over the kinetic effect. Note: in our model, ee_{oc} is zero in this situation since there are no D hydrophobic monomers that would otherwise be occluded.

TABLE VI: Orientation of floating glycine crystals by hydrophobic effect in the presence of resolved hydrophilic additives and 1% (w/w_{gly}) hydrophobic amino acids of the opposite configuration

| (D) | | | | | |
|-------------|----------------------|----------------------|------|------|-----------|
| Hydrophilic | $f + \bar{f}$ | P | od | ee | ee_{oc} |
| w/w_{gly} | $mol \cdot l^{-1}$ | $mol \cdot l^{-1}$ | (%) | (%) | (%) |
| 0.01 | $1.86 \cdot 10^{-3}$ | $4.26 \cdot 10^{-2}$ | 100 | 100 | 0 |
| 0.05 | $2.15 \cdot 10^{-4}$ | $4.42 \cdot 10^{-2}$ | 100 | 100 | 0 |
| 0.1 | $1.04 \cdot 10^{-4}$ | $4.43 \cdot 10^{-2}$ | 100 | 100 | 0 |
| 0.5 | $2.04 \cdot 10^{-4}$ | $4.44 \cdot 10^{-2}$ | 100 | 100 | 0 |

4. The amplification step

The hydrophobic resolved α -amino acids are advantageous for such a study with respect to the hydrophilic ones because both the kinetic inhibitory effect and the stabilization of the nuclei by hydrophobic effect act in the same direction for orientation of the growing floating crystals of glycine. For this reason, we next study the crystallization of glycine in the presence of partially enriched mixtures of (L,D)-hydrophobic amino acids at various concentrations.

The presence of an excess of hydrophobic (D)-amino acids will favor the (010) oriented nucleation at the interface while at the same time preventing the growth of (0 $\bar{1}$ 0) oriented crystals from the solution. The experimental[6] correlation between the initial enantiomeric excess of the solution with the total concentration needed to obtain complete orientation of the floating glycine crystals is reproduced here in Fig.5 for reference.

The correlation between the initial enantiomeric excess of the solution with the total concentration needed to obtain *maximum* orientation of the floating glycine crystals is shown in Fig. 6. In the Table VII we list all the *od* values obtained for the different initial enantiomeric excesses and concentrations, the numbers in boldface correspond to the maximum orientations and these are plotted in Fig. 6. The point we wish to illustrate here is simply that our model succeeds in capturing the general *trend* observed in the experiment, namely that smaller initial enantiomeric excesses require greater initial hydrophobic amino acid concentrations in order to achieve a (maximal) crystal orientation. Figure 7 shows the temporal evolution of this situation.

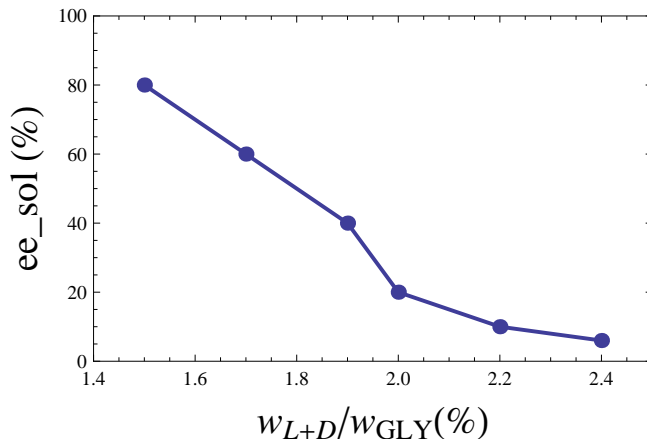


FIG. 5: Correlation between the initial leucine enantiomeric excess in solution and the total concentration needed for the complete $(0\bar{1}0)$ orientation of the floating glycine crystals. From reference[6].

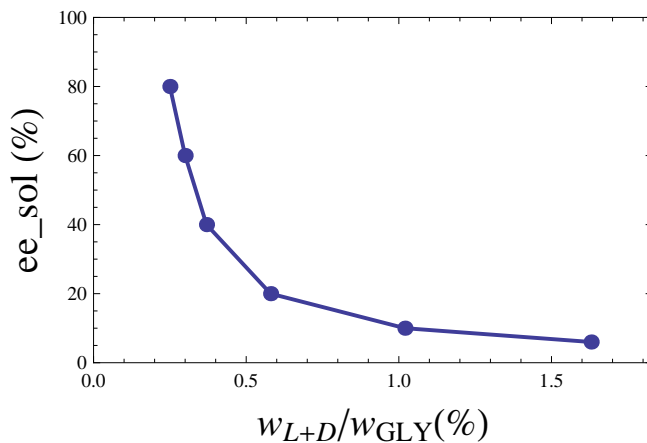


FIG. 6: Correlation between the initial enantiomeric excess of the hydrophobic additive in solution and the total concentration needed for the *maximal* $(0\bar{1}0)$ orientation of the floating glycine crystals. See Table VII and text for discussion.

Experimental proof that hydrophobic effect plays a dominant role in the orientation of the glycine crystals can be deduced from Table IV of reference[6]. Nevertheless, both effects are always present for the hydrophobic amino acids: those in solution contribute to the inhibitory kinetic effect, this is depicted in Figure 5. This also explains why, at higher concentrations, the glycine plates observed in the experiment are so thin. At lower initial *ee*, the higher concentrations needed appear to forbid formation of floating plates altogether[6].

VI. CONCLUSIONS AND DISCUSSION

We have presented a mathematical model for achieving resolution of racemic solutions of alpha-amino acids and glycine into enantiomeric territories based on a chemical scheme proposed by the Rehovot group some years ago. Their crystallization experiments provide a simple model for the generation and amplification of optically active amino acids

TABLE VII: Orientation degree od of floating glycine crystals in the presence of enriched mixture of hydrophobic additives. For each initial enantiomeric excess, a maximum degree of orientation is reached, to identify it we first locate the pair of values (the range) containing this maximum (bold font)

| $ee_0(\%)$ | w/w_{gly} | | | | | | | | |
|------------|-------------|--------------|--------------|--------------|--------------|--------------|--------------|-------|-------|
| | 0.001 | 0.002 | 0.003 | 0.004 | 0.005 | 0.006 | 0.007 | 0.008 | 0.009 |
| 6 | 69.81 | 74.28 | 76.63 | 78.18 | 79.34 | 80.28 | 81.08 | 81.78 | 82.4 |
| 10 | 79.71 | 83.18 | 85 | 86.2 | 87.09 | 87.81 | 88.41 | 88.92 | 89.38 |
| 20 | 90.3 | 92.34 | 93.38 | 94.06 | 94.55 | 94.82 | 94.51 | 94.25 | 94.02 |
| 40 | 96.97 | 97.77 | 98.16 | 98.28 | 98.11 | 97.97 | 97.85 | 97.74 | 97.64 |
| 60 | 99.03 | 99.35 | 99.47 | 99.41 | 99.36 | 99.32 | 99.28 | 99.24 | 99.21 |
| 80 | 99.77 | 99.86 | 99.88 | 99.87 | 99.87 | 99.86 | 99.85 | 99.85 | 99.84 |

| $ee_0(\%)$ | w/w_{gly} | | | | | | | | |
|------------|--------------|--------------|--------------|-------|-------|-------|-------|-------|-------|
| | 0.01 | 0.02 | 0.03 | 0.04 | 0.05 | 0.06 | 0.07 | 0.08 | 0.09 |
| 6 | 82.96 | 85.13 | 84.26 | 83.8 | 83.52 | 83.35 | 83.24 | 83.16 | 83.11 |
| 10 | 89.79 | 88.18 | 87.46 | 87.09 | 86.86 | 86.72 | 86.63 | 86.57 | 86.53 |
| 20 | 93.82 | 92.7 | 92.22 | 91.97 | 91.81 | 91.72 | 91.65 | 91.61 | 91.58 |
| 40 | 97.56 | 97.05 | 96.81 | 96.68 | 96.6 | 96.54 | 96.5 | 96.48 | 96.46 |
| 60 | 99.18 | 98.99 | 98.89 | 98.82 | 98.78 | 98.75 | 98.73 | 98.71 | 98.7 |
| 80 | 99.84 | 99.8 | 99.78 | 99.76 | 99.75 | 99.74 | 99.74 | 99.73 | 99.72 |

TABLE VIII: Maximum orientation degree od of floating glycine crystals in the presence of enriched mixture of hydrophobic additives for each initial enantiomeric excess

| $ee_0(\%)$ | 6 | 10 | 20 | 40 | 60 | 80 |
|-------------|--------|--------|--------|--------|-------|--------|
| w/w_{gly} | 0.0163 | 0.0102 | 0.0058 | 0.0037 | 0.003 | 0.0025 |

in prebiotic conditions. The glycine and alpha amino acid system may be relevant to the origin of optical activity as it involves compounds that are among the simplest building blocks of life. In this vein it is interesting to point out that a recent prebiotic synthesis of protobiopolymers under alkaline ocean conditions has yielded a variety of amino acids with glycine being the most abundant[9]. In an astrophysical context, amino acids have been detected in room-temperature residues of UV-irradiated interstellar ice analogues, and again glycine was found to be the most abundant amino acid[16].

Centrosymmetric glycine crystals were employed as substrates for the total separation of occluded alpha-amino acids into enantiomeric territories. These amino acid additives are occluded enantioselectively through the enantiotopic (010) and (0 $\bar{1}$ 0) faces of the glycine crystals. Such crystals when floating at the air/solution interface, and if properly oriented, may incorporate only one of the two enantiomer additives present in the solution. Complete (010) or (0 $\bar{1}$ 0) orientation is induced by both a kinetic and a hydrophobic effect. The former effect acts through an inhibition of the nucleation and growth of that enantiomorph which interacts with the resolved additive. The latter effect is due to the induction of a specific enantiotopic face orientation (e.g., (0 $\bar{1}$ 0) exposed toward the solution) by the hydrophobic amino acids at the interface. Combination of both effects acts in the same direction driving exclusive orientation of the glycine crystals and thus triggers an amplification starting from an initial random oriented crystal and a solution with low initial enantiomeric excess. This is represented schematically by Figure 1. Our mathematical model results from translating this scheme into basic reaction steps and then into a corresponding system of differential rate equations which we then simulate to test out the hypothesized mechanisms and to underscore the salient features of the original experiment.

Our immediate goal here is to capture the essential mechanisms responsible for the symmetry breaking in the simplest terms possible. This has led us to make certain simplifications, in keeping with this aim. A major simplification is to adopt reaction rates that are independent of the instantaneous size of the glycine crystal and of the number of occluded amino acid guest monomers. Another simplification is to model the processes without using explicit coordinate dependence, which otherwise would have necessitated the introduction of partial derivatives, diffusion constants, spatially dependent concentrations and a coordinate system that distinguishes the bulk three dimensional solution from the bounding two-dimensional air/water interface or layer. There is no doubt that these *spatial* aspects play a supporting role in the actual experiment, but they are not the primary *cause* of the mirror symmetry breaking observed there. The fact that the coordinate-free model leads to chiral symmetry breaking and to the territorial separation of the enantiomers is proof of this. We have provided an analytic linear stability analysis which gives inde-

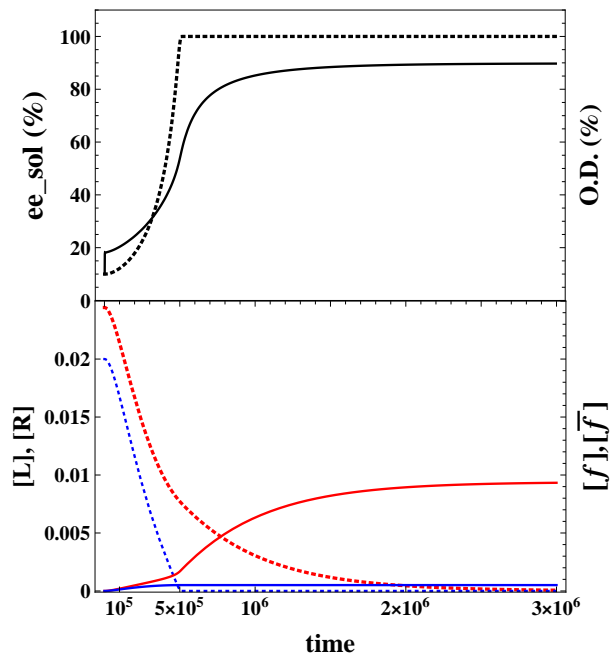


FIG. 7: Partially enriched mixtures of (L,D)-hydrophobic amino acids. Initial conditions: $ee_0 = 0.1$, $w/w_{gly} = 0.01$, $ee_h0 = 0$, $w_h/w_{gly} = 0$. Upper figure: the orientation degree od (solid line) and the enantiomeric excess ee in solution (dotted line). Lower figure : concentration of the hydrophobic monomers (the upper dotted curve is $[L]$). Solid lines represent the concentration of oriented crystals ($[f]$ is the upper curve).

pendent confirmation of this. The mathematical model leads to separation of enantiomeric territories, the generation and amplification of optical activity by enantioselective occlusion of chiral additives through chiral surfaces of glycine crystals.

We emphasized earlier the experimentally remarkable feature that the chemical system does away with the need for mechanical energy for achieving the amplification of the ee of the amino acids in solution. To this end we can identify an aspect of the experiment that serves as an effective "driving force" that maintains the system out of equilibrium, a seemingly necessary condition for the (permanent [24]) breaking of mirror symmetry. Indeed, the experiment requires supersaturated solutions of glycine. To achieve supersaturation, the system must be (i) cooled down and/or (ii) the solvent must evaporate. This then adds the element of irreversibility.

Recent works related to the original experimental model we consider here are summarized in a current review of the role of crystalline architectures as templates relevant for the origins of homochirality [12]. In brief, similar stochastic separation of α -amino acids has also been achieved when racemic alpha-amino acids are occluded within enantiomorphous β -glycine crystals [17]. When this form is grown in either porous materials[18, 19] or small solution volumes[20], the beta polymorph glycine crystallizes as long needles. When the β -form is grown in the presence of DL-amino acids, the L-molecules are occluded only in one of the β -glycine enantiomorphs, while the D's are occluded only in the other. Thus, if a small number of one the β enantiomorphs crystallizes first, they will occlude only one of the alpha amino acid enantiomers, thereby enriching the solution in the other amino acid. This excess should prevent the nucleation of fresh β -Gly crystals of the opposite handedness and thus lead to an enrichment of the ee of the amino acids in solution.

The present model is much simplified with respect to the actual experimental situation in solution. It is therefore worthwhile to identify potential future efforts aimed at "dressing" this minimal model so as to increase its relative "complexity", only of course when this is warranted or justified experimentally. One such effort we are currently investigating is a more realistic modeling of the self-assembly of the hydrophobic amino acid monolayer[7] at the air/water interface and its role in precipitating the oriented glycine crystals. Further theoretical work aimed at incorporating other physical and chemical aspects to the underlying scheme could also include, for example, mass transport and diffusion, and a detailed modeling of the the glycine crust formed at the interface. We hope to report results along these lines elsewhere.

Acknowledgements

The ESF COST Action CM0703 "Systems Chemistry" supported a visit of Meir Lahav to DH at the Centro de Astrobiología in Madrid and we also thank Josep Ribó who participated in the initial discussions and helped to foment this collaboration. We are grateful to Meir Lahav for encouraging us to propose a mathematical model for these experiments and for many helpful discussions and correspondence during the course of this work. CB has a Calvo-Rodés predoctoral scholarship from the Instituto Nacional de Técnica Aeroespacial (INTA) and the research of DH is supported in part by the grant AYA2009-13920-C02-01 from the Ministerio de Ciencia e Innovación (Spain) and forms part of the above-mentioned COST Action. Thanks to Marta Ruiz-Bermejo for supplying us with the references on glycine abundance in prebiotic synthesis experiments and in simulations of interstellar ice analogues.

-
- [1] A. Guijarro and M. Yus, *The Origin of Chirality in the Molecules of Life* (RSC Publishing, Cambridge, 2009), 1st ed.
 - [2] D. Kondepudi, I. Prigogine, and G. Nelson, *Phys. Lett. A* **111**, 29 (1985).
 - [3] V. Avetisov, V. Kuz'min, and S. Anikin, *Chem. Phys.* **112**, 179 (1987).
 - [4] I. Weissbuch, L. Leiserowitz, and M. Lahav, *Top. Curr. Chem.* **259**, 123 (2005).
 - [5] I. Weissbuch, L. Addadi, Z. Berkovitch-Yellin, E. Gati, M. Lahav, and L. Leiserowitz, *Nature* **310**, 161 (1984).
 - [6] I. Weissbuch, L. Addadi, L. Leiserowitz, and M. Lahav, *J. Am. Chem. Soc.* **110**, 561 (1988).
 - [7] E. Landau, S. G. Wolf, M. Levanon, L. Leiserowitz, M. Lahav, and J. Sagiv, *J. Am. Chem. Soc.* **111**, 1436 (1989).
 - [8] I. Weissbuch, M. Lahav, and L. Leiserowitz, *Cryst. Growth Des.* **3**, 125 (2003).
 - [9] M. Ruiz-Bermejo, L. Rivas, A. Palacín, C. Menor-Salván, and S. Osuna-Esteban, *Orig. Life Evol. Biosph.* (2010).
 - [10] D. Kondepudi, R. Kaufman, and N. Singh, *Science* **250**, 975 (1990).
 - [11] C. Viedma, *Phys. Rev. Lett.* **94**, 065504 (2005).
 - [12] I. Weissbuch and M. Lahav, *Chem. Rev.* **111**(5), 3236 (2011).
 - [13] K. Mislow, *Collect. Czech. Chem. Commun.* **68**, 849 (2003).
 - [14] I. Weissbuch, V. Y. Torbeev, L. Leiserowitz, and M. Lahav, *Angew. Chem. Int. Ed.* **44**, 3226 (2005).
 - [15] S. G. Wolf, L. Leiserowitz, M. Lahav, M. Deutsch, K. Kjaer, and J. Als-Nielsen, *Nature* **328**, 63 (1987).
 - [16] G. Muñoz Caro, U. Meierhenrich, W. Schutte, B. Barbier, A. Arcones Segovia, H. Rosenbauer, W. H.-P. Thiemann, A. Brack, and J. Greenberg, *Nature* **416**, 403 (2002).
 - [17] V. Torbeev, E. Shavit, I. Weissbuch, L. Leiserowitz, and M. Lahav, *Cryst. Growth Des.* **5**, 2190 (2005).
 - [18] B. Hamilton, M. Hillmyer, and M. Ward, *Cryst. Growth Des.* **8**, 3368 (2008).
 - [19] B. Hamilton, I. Weissbuch, M. Lahav, M. Hillmyer, and M. Ward, *J. Am. Chem. Soc.* **131**, 2588 (2009).
 - [20] A. Lee, I. Lee, S. Dette, J. Boerner, and A. Myerson, *J. Am. Chem. Soc.* **127**, 14982 (2005).
 - [21] J. Crusats, D. Hochberg, A. Moyano, and J. Ribó, *ChemPhysChem.* **10**, 2123 (2009).
 - [22] C. Blanco, M. Stich, and D. Hochberg, *Chem. Phys. Lett.* **505**, 140 (2011).
 - [23] In the original Hebrew version of the Bible, *adam* stands for all members of mankind: man, woman, boy or girl. So there are two "Adams" in the Hebrew language, (i) Adam denoting Mankind and so implicitly including *both sexes*, as distinct from (ii) Adam the male, who was differentiated from Eve the female. We use the first definition as a metaphor for the formation of the first glycine crystal, where both potential interface orientations are implicit, instead of Eve, which might represent a secondary crystallization.
 - [24] *Temporary* breaking of mirror or chiral symmetry is however possible even for closed systems in thermodynamic equilibrium, see for example recent simulations of the reversible Frank model closed to matter and energy flow.[21, 22]